Oral Lichen Planus Classification Using Auto Associative Neural Network

Dr. C. Kalyani (MDS)[1],Dr. S. Venkatakrishnan[2], P. Dhanalakshmi[3]
[1]Dept of Oral Pathology and Microbiology, RMDCH, Annamalai University,Annamalainagar,Tamilnadu,India
[2] Engineering Wing, Annamalai University,Annamalainagar,Tamilnadu,India.
[3] Associate Professor, Department of CSE, Annamalai University,Annamalainagar,Tamilnadu,India.

Abstract-*Oral Lichen Planus is an ongoing chronic inflammatory condition that affects mucous membranes inside the mouth. Oral lichen planus may appear as white, lacy patches; red, swollen tissues; or open sores. These lesions may cause burning, pain or other discomfort. In this work, microscopic images of normal and OLP are taken. Block Intensity Comparison Code and histogram are used for feature extraction. Auto Associative Neural Network is used for classification of Oral Lichen planus from normal.*

Keywords-Block Intensity Code Comparison (BICC), Auto Associative Neural Network (AANN), Oral Lichen planus(OLP), Oral Squamous Cell Carcinoma (OSCC)

I. INTRODUCTION

Lichen Planus is another common precancerous lesion. It can occur in the skin and in the oral cavity, hence called as mucocutaneous lesion. Lichen Planus is a mucocutaneous disease, characterized by an unspecific chronic inflammatory process, which leads to an intense destruction of the basal layer of the epithelium. Lichen planus affects from 1% to 2% of the population, being the most frequent dermatological disease that involves the oral cavity [1].

The malignant potential of Oral Lichen Planus (OLP) provided clinical evidence that patients affected by OLP have an increased risk to develop Oral Squamous Cell Carcinoma (OSCC); nevertheless, controversies still exist as to whether OLP has inherent predisposition to become malignant, or not [2].

Oral Lichen Planus (OLP) is a chronic inflammatory disease of unknown etiology [1]. Oral lichen planus presents as white striations, white papules, white plaques, erythema, erosions or blisters affecting predominantly the buccal mucosa, tongue and gingivae, although other sites are occasionally involved. Oral lichen planus affects 1-2 per cent of the general adult population and is the most common non-infectious oral mucosal disease. Oral lichen planus affects women more than men (1.4:1). Oral lichen planus occurs predominantly in adults over 40, although younger adults and children may be affected. Lesions are typically bilateral and often appear as a mixture of clinical subtypes. White or grey streaks may form a linear or reticular pattern on an erythematous background. Alternatively, there may be a central area of shallow ulceration (erosion) with a yellowish surface (fibrinous exudate) surrounded by an area of erythema. Notwithstanding the multiple oral manifestations that form the basis of most current clinical classifications of OLP, the major issue is to arrive at a correct diagnosis. OLP can present itself as any of the following forms- ulcer, plaque. Patch, erosion, papules, etc. Almost all cases of OLP present with reticular keratotic [white] striae in some area of the oral mucosa [3].

World Health Organization has defined OLP as a potentially precancerous disorder, representing a generalized state associated with a significantly increased risk of cancer. However, only 0.5 - 2.9% of OLP lesions will progress to cancer [5].

Lichen planus is a T-cell-mediated autoimmune disease in which autocytotoxic CD8+T cells trigger apoptosis of oral epithelial cells. Histopathologic examination of lesional tissue is the most relevant investigation in cases of oral lichen planus. Consistent findings include a bandlike subepithelial mononuclear infiltrate consisting of T cells and histiocytes, increased numbers of intraepithelial T cells, and degenerating basal keratinocytes that form colloid (civatte, hyaline, cytoid) bodies, which appear as homogenous eosinophilic globules. Variable findings include parakeratosis, acanthosis, and sawtooth rete pegs. Degeneration of the basal keratinocytes and disruption of the anchoring elements of the epithelial basement membrane and basal keratinocytes (eg, hemidesmosomes, filaments, fibrils) weakens the epithelial-connective tissue interface. As a result, histologic clefts (ie, Max- Joseph spaces) may form, and blisters on the oral mucosa (bullous lichen planus) may be seen at clinical examination. B cells and plasma cells are uncommon findings [4].

Fig.1 (a): shows the white radiating striae characteristic of OLP in the inner side of the cheek. Fig. 1 (b): shows a similar lesion seen on the lateral side of the tongue. Fig .2: shows a similar lesion on the gingiva.

(a)

(b)

Fig. 1: (a) Lichen Planus of cheek mucosa, (b) Lichen Planus of tongue

(c)

Fig. 2: Lichen Planus of Gingiva (gums)

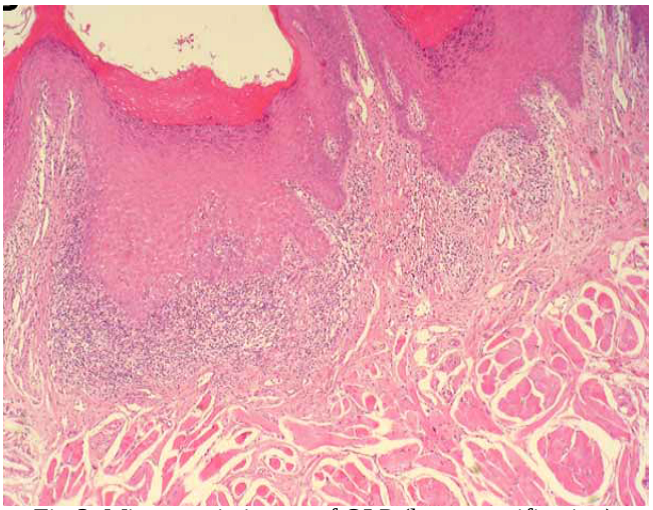

Fig.3: Microscopic image of OLP (low magnification)

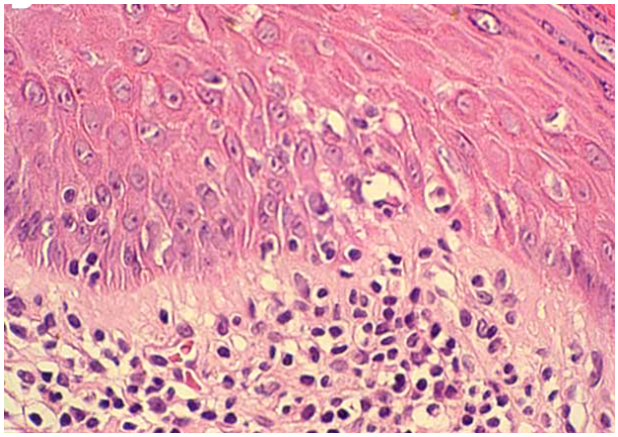

Fig. 4 : OLP image under high magnification

Fig. 3: shows the appearance of a Lichen planus lesion under microscope. The epithelium is hyperplastic and the connective tissue shows inflammatory cell accumulation. Fig. 4: shows the same lesion under high magnification.

II. FEATURE EXTRACTION

Color histogram features as are extracted from both OLP affected and normal images. BICC features such as from both OLP affected and normal images. The features are combined and normalized using equation to produce a feature vector which characterizes the image.

$$y_i = \frac{(x_i - x_{min})}{x_{max} - x_{min}}$$

where x_{max} and x_{min} are the maximum and the minimum values X_i of the un normalized data using Histogram features were extracted for 16, 32, 64 bins and BICC features were extracted for blocks of size 5 x 5, 10 x 10, 15 x 15 which resulted in 10, 45, 105 dimensional feature vectors respectively.

B. Architecture of Auto Associative Neural Network Models

A special kind of back propagation neural network called Auto associative Neural Network (AANN) can be used to capture the distribution of feature vectors in the feature space.

Autoassociative Neural Network models are feed forward neural networks performing an identity mapping of the input space and are used to capture the distribution of the input data. The distribution capturing ability of the AANN model is described in this section.

The five layer AANN model shown in Fig. 3, which has three hidden layers. In this network, the second and fourth layers have more units than the input layer. The third layer has

fewer units than the first or fifth. The processing units in the first and third hidden layer are nonlinear and the units in the third compression/hidden layer can be linear or nonlinear. As the error between the actual and the desired output vectors is minimized, the cluster of points in the input space determines the shape of the hyper surface obtained by the projection onto the lower dimensional space.

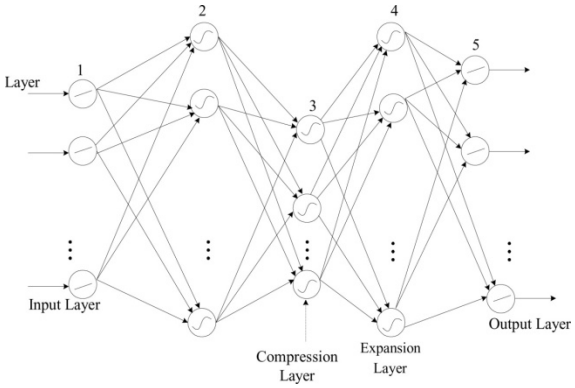

Fig. 5: A Five Layer AANN Model

III. EXPERIMENTAL RESULTS

A. Database

A total of 200 microscopic images which consists of 100 OLP images and 100 normal images are considered. For four fold cross validation training data gf_i (i=1, 2, 3, 4) consisting of 150 microscopic images [50 images (25 Normal + 25 OLP) + 50 images (25 Normal + 25 OLP) + 50 images (25 Normal + 25 OLP)] are used. For testing, 50 microscopic images (25 Normal and 25 OLP) are used.

AANN models perform an identical mapping of the input space. The distribution of 16, 32 and 64 histogram bins and 10, 45 and 105 dimensional feature vectors in the feature space for different sized blocks of BICC feature vectors is captured using an AANN model. Separate AANN models are used to capture the distribution of feature vectors of each class and the network is trained for 500 epochs. One epoch of training is a single presentation of all the training vectors to the network.

B. Performance Measures

For evaluating the performance of the system, the feature vector is given as input to each of the models. The output of the model is compared with the input to compute the normalized squared error. The normalized squared error (E) for the feature vector y is given by, $E = \frac{||y-o||^2}{||y||^2}$, where ***o*** is the output vector given by the model. The error (E) is transformed into a confidence score (C) using C = exp (E). The average confidence score is calculated for each model. The class is decided based on the highest confidence score. The performance of the system is evaluated, and the method achieves 96.0% classification rate. The structure of AANN model plays an important role in capturing the distribution of the feature vectors. After some trial and error, the network structure 105L - 210N - 50N - 210N - 105L is obtained. This structure seems to give good performance in terms of classification accuracy. For testing, the feature vectors extracted from the various images are given as input to the model and the corresponding class has the maximum confidence score. The performance results are shown in Tables 1, 2 and 3 for Histogram, BICC and combined features respectively.

Table 1: Average performance of normal and OLP Classification by AANN model usingHistogram features.

Structure of AANN	Accuracy (%)					
	Feature vector dimensions (No. of bins)					
	16		32		64	
	Normal	OLP	Normal	OLP	Normal	OLP
16L - 76N - 2N - 76N - 16L	82.1	85.0	86.0	88.8	87.8	90.6
32L - 76N - 4N - 76N - 32L	84.3	86.4	87.6	89.8	88.6	91.5
64L - 128N - 6N - 128N - 64L	88.2	89.4	87.9	91.6	91.0	93.6

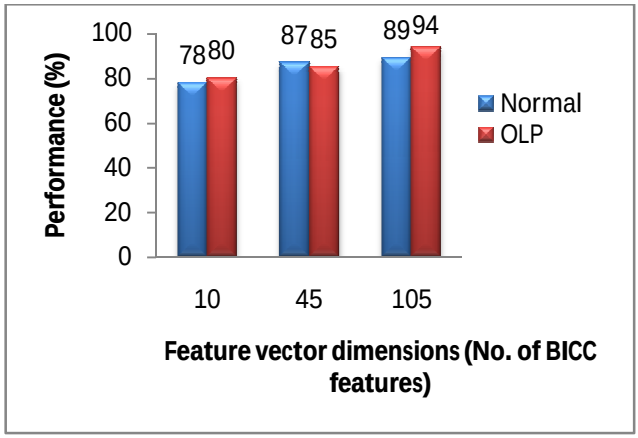

Fig. 6: Average performance of normal and OLP classification by AANN model with the structure 64L - 128N - 6N - 128N - 64L using Histogram features

Table 2: Average performance of normal and OLP classification by AANN model using BICC features.

Structure of AANN	Accuracy (%)					
	Feature vector dimensions (No. of BICC features)					
	10		45		105	
	Normal	OLP	Normal	OLP	Normal	OLP
10L - 12N - 3N -12N - 10L	82.4	86.4	86.5	88.0	89.3	90.0
45L - 78N - 12N - 78N - 45L	83.1	88.6	89.4	91.5	90.9	93.4
105L - 210N - 60N - 210N - 105L	87.8	90.1	91.0	93.6	93.4	95.2

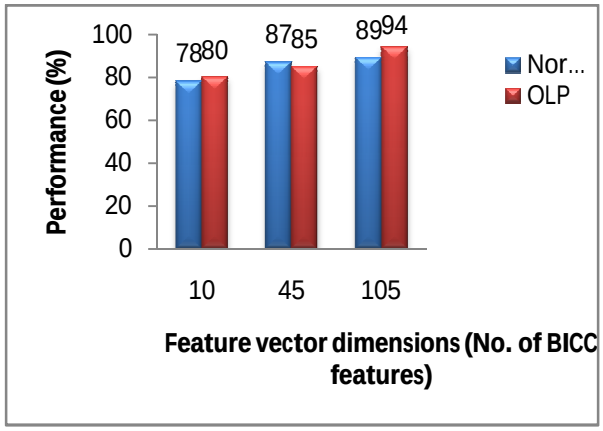

Fig. 7: Average performance of normal and OLP classification by AANN model with 105L - 210N - 50N - 210N - 105L using BICC features.

Table 3: Average performance of normal and OLP classification by AANN model using combined features.

Structure of AANN	Accuracy (%)					
	No. of combined features (Histogram + BICC)					
	26		77		169	
	Normal	OLP	Normal	OLP	Normal	OLP
26L - 52N - 4N - 52N - 26L	68.4	71.6	70.2	72.6	74.6	76.1
77L - 96N - 22N - 96N - 77L	90.9	92.5	93.0	94.5	93.5	96.0
169L - 340N - 35N - 340N -169L	87.0	90.0	91.8	93.3	93.4	95.0

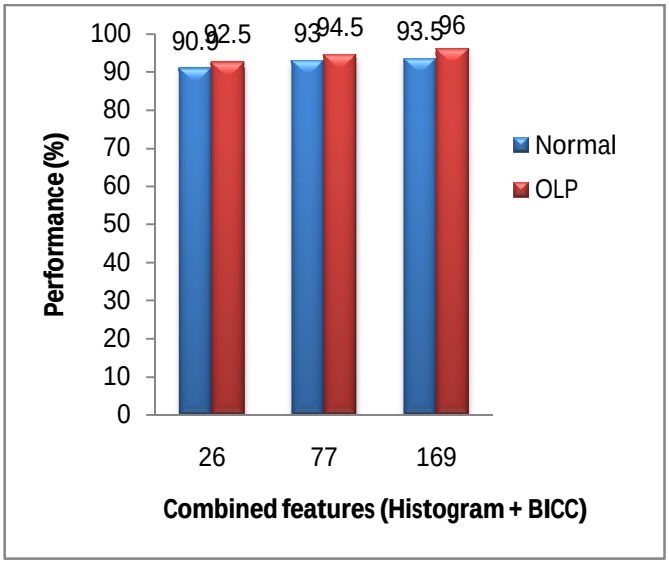

Fig. 8: Average performance of normal and OLP classification by AANN model with 77L - 96N - 22N - 96N - 77L using combined features.

The number of units in the third layer (compression layer) determines the number of components captured by the network. The AANN model projects the input vectors onto the subspace spanned by the number of units (n_c) in the compression layer. If there are n_c units in the compression layer, then the BICC feature vectors are projected onto the subspace spanned by n_c components to realize them at the output layer. The effect of changing the value of n_c on the performance of OLP classification is studied. Various structures were experimented and finally the structure 77L - 96N - 22N - 96N - 77L shows optimal performance for the combined features.

IV. CONCLUSION

The performance of OLP using AANN has been analyzed. BICC features and histogram features are extracted to characterize the OLP images. Experimental results show that the proposed OLP classification scheme is very effective with an accuracy rate of above 90.0 AANN shows the highest accuracy of 96% for OLP classification, with 169 combined features.

REFERENCES

[1] Mussarat Yasmin, Muhammad Sharif and Sajjad Mohsin, “Survey Paper on Diagnosis of Breast Cancer Using Image Processing Techniques”, Research Journal of Recent Sciences, vol. 2, no. 10, pp. 88-98, October 2013.

[2] Mignogna M. D., Lo Muzio L, Lo Russo L, Fedele S, Ruoppo E and Bucci E, “Clinical guidelines in early

detection of oral squamous cell carcinoma arising in oral lichen planus: a 5-year experience", Oral Oncology, vol.37, no. 3, pp. 262-267, April 2001.

[3] Sugerman P. B and Savage N. W, "Oral lichen planus: causes, diagnosis and management", Australian Dental Journal, vol. 47, no. 4, pp. 290-7, December 2002.

[4] Furkan Keskin, Alexander Suhre, Kivanc Kose, Tulin Ersahin, Enis Cetin A and Rengul Cetin-Atalay, "Image Classification of Human Carcinoma Cells Using Complex Wavelet-Based Covariance Descriptors", PLoS ONE, vol. 8, no. 1, p. 52807, January 2013.

[5] Riikka Mattila, "Molecular Markers of Oral Lichen Planus", Ph.D. thesis, Medica – Odontologica, 2009.

[6] Fernando Augusto C, Garcia de Sousa, Paradella and Thas Cachut, "Malignant potential of oral lichen planus: A meta-analysis", Revista Odonto Ciência (Journal of Dental Science), vol. 24, no. 2, pp. 194-197, February 2009.

[7] Chandan Gautam, Vadlamani Ravi," Counter propagation auto associative neural network based data imputation", Elsevier, Volume 325,page 288-299,December 2015.

[8] Bruno J.T. Fernandes, George D.C. Cavalcanti " Auto Associative Pyramidal Neural Network for one class pattern classification with implicit feature extraction" September 2015.